

COB-2023-0444

THERMAL ANALYSIS OF THE IMPACT OF SIX MONTHS IN A 1U CUBESAT IN LEO

Rodrigo da Silva Cardozo^[1]

[1] Federal University of Santa Catarina. Technological Center of Joinville. R. D. Francisca 8300, Joinville - SC, 89218-000
rodrigodasilvacardozo@gmail.com

Damylle Cristina Xavier Donati^[1]

damylle.xavier@t2f.ufsc.br

Talita Sauter Possamai^[1]

talita.possamai@ufsc.br

Renato Oba^[1]

renato.oba@ufsc.br

Abstract.

Space projects, especially orbital platform projects, are comprised of high investment costs, requiring rigorous analysis in their development. The operating conditions of such devices include sudden changes in external temperature as a result of incident radiation during orbit, heat generation in electronic devices, and heat conduction for thermal control of subsystems. Nanosatellite development teams commonly have limited access to robust mission analysis and thermal analysis tools, such as environmental testing, numerical simulation software, and mission design software, due to low budgets when compared to large satellites. For this reason, simplified models of thermal analysis are used to define critical mission requirements. However, there is great difficulty in coupling thermal and orbit requirements, as they are independent complex phenomena. The present work aims to develop a thermal analysis module based on a lumped heat transfer model to be applied as an add-on module to an open-source orbital mission analysis code. The module is validated with the aid of literature data for fixed Beta angles comparing incident radiation on each face of the satellite. For a Beta angle of 0° and 72°, the incident solar, albedo, and infrared radiation on the six faces of a 1U CubeSat in LEO (Low Earth Orbit) are consistent with published data from different authors found in the literature. An analysis of the implications of the variation of the Beta angle in LEO for a 1U CubeSat in six months in orbit time is then presented indicating that without a propulsion system is expected that a 1U CubeSat variates its Beta angle between -72° to 72° in approximately 6 months in LEO. This variation results in an average total incident radiation of approximately 30% in the analyzed period. For the temperatures in each face, variations of more than 30 K can be seen for some faces while variations of 20 to 30 K can be seen for the Printed Circuit Board (PCB).

Keywords: Space radiation, CubeSat, Nanosatellite, Thermal transfer

1. INTRODUCTION

With the advance of the New Space sector and nanosatellites in these last years, the development of this type of space system for research and commercial applications by universities, research centers, and small to medium companies was made possible due to lower cost and faster financial feedback. (Bousedra, 2023, Tucker et al., 2023, Paravano et al., 2023)

CubeSats are standardized nanosatellites with 10x10x10 cm that usually operate in Low Earth Orbit (LEO) in thermal cycles of 70 to 100 minutes while orbiting around Earth (Garzón et al., 2022; Bonnici et al., 2019; Morsch Filho et al., (2021). During these cycles, the satellite can receive direct solar radiation during a period and then be in the eclipse area behind Earth within less than 60 minutes. This continuous cycle of incident radiation may result in significant temperature variation of the components of the satellite through its life cycle outside its operational range thus generating a possible critical failure of the system. Until 2018, 21% of the total of approximately 1,000 CubeSats launched reported total failure of the space system for reasons that comprise different subsystems and possible causes (Villela et al., 2019). Since temperature is a parameter that affects all subsystems correct prediction and control are important for the success of the mission.

This correct prediction of temperature in the CubeSat is dependent on at least two complex and connected phenomena: the orbital propagation of the satellite and its dynamic movement and space radiation based on the position of each face of the satellite in orbit. Currently, numerical modeling for the prediction of orbital and thermal control in CubeSats can be accomplished through commercial software developed for classical space systems such as large satellites.

However, its accessibility for small companies and universities is restricted due to the cost of this software. Another option for this portion of developers is to develop a model capable of predicting the orbital and thermal behavior of

CubeSats, as accomplished by Olatunji et al. (2022), Bonnici et al. (2019), Ali et al. (2017). Due to the complexity of the modeling, each author applies simplifications and hypotheses related to their objectives. One of these simplifications is the consideration of an orbital behavior of the nanosatellite based on a fixed beta angle through the whole orbit analyzed. In reality, due to the lack of an active propulsion system and active attitude control in most CubeSats, this angle varies significantly within the year due to a combination of orbital parameters and the relative position of the Sun and Earth (Garzón et al., 2022) going from 0 to 72°.

The objective of this work is to analyze the effect of the variation of the Beta angle on the temperatures of a 1U CubeSat in LEO through a thermal lumped model coupled to an orbital and incident radiation algorithm developed in-house and validated based on literature data for incident radiation for classical fixed Betas angles.

2. METHODOLOGY

2.1. Orbit propagation model and dynamic of the satellite

The incident radiation on each face of the CubeSat is related to the orbital position of the satellite through the beta angle (β), defined as the angle between the orbit plane of the satellite and the position of the sun. This relation is presented in Figure 1 (a) and mathematically calculated by equation (1):

$$\beta = \arcsin \left[\cos(\Gamma) \sin(\Omega) \sin(i) - \sin(\Gamma) \cos(\epsilon) \cos(\Omega) \sin(i) + \sin(\Gamma) \sin(\epsilon) \cos(\Omega) \cos(i) \right], \quad (1)$$

where Γ is the eclipse's true solar longitude, Ω is the ascending node length, i is the orbit inclination, and ϵ the axial inclination of the Earth. The last one varies little with time and currently, its value is approximately 23,45°.

The propagation of the orbit model applies the Gaussian variational equations (Curtis, 2014). The six parameters considered in the integration of the second law of Newton are the specific angular momentum (h), the inclination (i), the ascending node length (Ω), the eccentricity (e), the perigee argument (ω) and the true anomaly (θ). Each parameter is indicated in Figure 1 (b). The perturbations related to the gravitational force of Earth (J2) and atmosphere drag were considered as perturbations based on Capderou et al. (20214) which indicates that for altitudes below 2000 km, these two perturbations are the most significant. The drag coefficient of 2.2 was applied (Curtis, 2014) while the NRLMSISE-00 atmosphere model developed by the US Naval Research Laboratory and presented by Picone et al. (2002) was employed for the data of the atmospheric density.

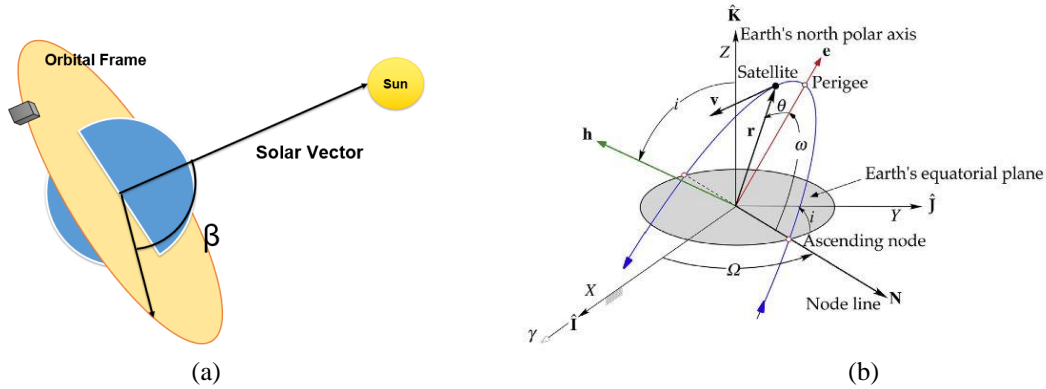


Figure 1. (a) Definition of Beta angle and (b) Kepler Orbital Parameters (Curtis, 2014).

The gravitational force of the Earth model (J2) considers the effect of the flattening of the polos and the widening at the equator. A movement model for the satellite-based on quaternions is integrated into the orbit propagation model to estimate the dynamic of the CubeSat.

2.2. Incident radiation model

The data generated by the orbit propagation model and by the dynamic model of the satellite is applied to calculate the irradiative heat flux related to each face of the CubeSat. Three radiative heat fluxes are considered: direct solar radiation, albedo radiation, and infrared radiation from Earth. Due to the geometric configuration of a CubeSat being always composed of a cube with external faces comprised of solar panels (except for the face occupied by the payload) or a combination of cubes, each face of the CubeSat can receive a combination of the irradiative heat flux indicated depending on its position and movement of the satellite. A radiative form factor is calculated for each face about the sun

vector (for direct sun irradiation) and about the Earth (for albedo irradiation and infrared irradiation) by applying the equations presented in (Nogueira et al., 2017).

The direct sun irradiation is estimated by equation (2)

$$Q_s = \alpha_s A_i \cos(b_i) I_s B_s, \quad (2)$$

where I_s is the direct sun irradiation flux (prescribed here as 1367 W/m^2), α_s is the absorptivity of the surface in the solar radiation spectrum, b_i is the angle between the surface and the solar radiative vector, and B_s is a nondimensional parameter that assumes the value of 1 when the face is being illuminated by the sun and the value zero when the face is located in the shadow of the Earth. The angle b_i is calculated by:

$$\cos(b_i) = \frac{\vec{H}_s \cdot \vec{N}_i}{|\vec{H}_s|}, \quad (3)$$

where \vec{H}_s is the solar radiation vector and \vec{N}_i is the unitary area vector from the face of the satellite.

The albedo radiation is dependent on the radiation form factor between Earth and the selected face of the satellite, F_{S-E} , the satellite surface absorptivity in the solar radiation spectrum, α_s , and a factor of reflected radiation by the Earth, γ_i , and is calculated by

$$Q_{alb} = \alpha_s A_i \gamma_i I_s F_{S-E}, \quad (4)$$

where the Earth's surface is considered a gray surface for the sun's radiation spectrum. For the infrared radiation emitted by the Earth's surface, the Earth is then considered a blackbody in the infrared radiation spectrum, and its emitted radiation is given by

$$Q_{IR} = \alpha_{IR} A_i I_E F_{S-E}, \quad (5)$$

where α_{IR} is now the absorptivity coefficient of the satellite face in the infrared radiation spectrum. The total incident radiation in each face of the satellite is then given by the sum of each radiation portion at each selected orbital position,

$$Q_{tot} = Q_s + Q_{alb} + Q_{IR}. \quad (6)$$

2.3. Thermal lumped model of the satellite

A classical lumped model as described by Bonnici et al. (2019) was applied for the thermal modeling of the satellite, based on the finite differences numerical approach with an explicit method for the temporal discretization. The model accounts for thermal contact resistances between each surface of the satellite. A total of 66 nodes were applied for the geometric model of a 1U CubeSat, presented in Figures 2 and 3, where 16 nodes were applied to the solar panels (Figure 2 (a)), 8 nodes for the vertical structures (in red in Figure 2 (a)), 16 nodes for the horizontal structures (in light and dark blue in Figure 2 (a)), 20 for connection bolts, 4 for PCBs (blue plates in Figure 2 (a)) and 2 for the top and bottom surface (pink plates in Figure 2 (b)). Figure 2 (b) shows the CubeSat with all the components assembled.

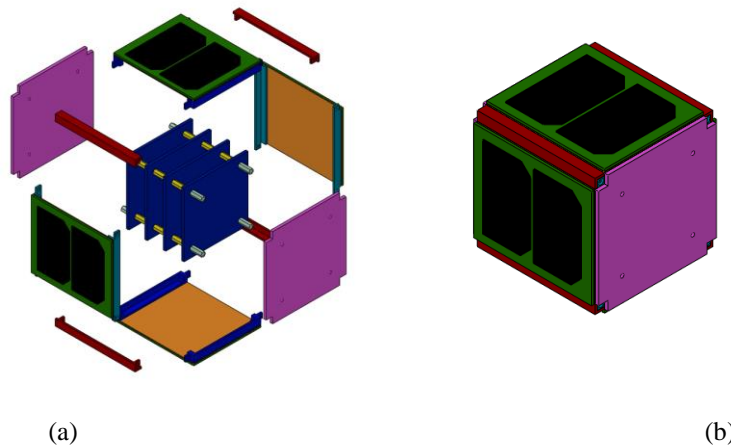


Figure 2. (a) Exploded view of Cubesat (b) Cubesat assembled.

2.4. Orbital and thermal parameters analyzed

The satellite is composed of four solar panels made of FR-4.0 with two silicon substrates, two aluminum plates 7075 (one at the superior face of the satellite and one at the bottom face of the satellite), four vertical structures and eight horizontal structures made of aluminum 7075, four FR-4.0 PCBs and twenty aluminum 7075 connections bolts. Table 1 lists the thermal properties of the materials, such as emissivity (ϵ), absorptivity (α), thermal conductivity (k), density (ρ) and specific heat (cp).

Table 1. Thermal properties of the materials applied to the thermal lumped model of the CubeSat.

Component	ϵ	α	k [W/m.K]	ρ [kg/m3]	cp [W/kg.K]	Material
Substrate	0.557	0.578	148.9	2330	712	Silicon
Panel Base	0.76	0.7	0.81	1850	1100	FR-4.0
Panel Base 2	0.3	0.13	121.2	2770	961	Aluminum 7075
Upper/Botton	0.3	0.13	121.2	2770	961	Aluminum 7075
PCB	0.76	0.07	0.81	1850	1100	FR-4.0
Vertical Structure	0.3	0.13	121.2	2770	961	Aluminum 7075
Horizontal Structure	0.3	0.13	121.2	2770	961	Aluminum 7075
Bolts	0.3	0.13	121.2	2770	961	Aluminum 7075

For results of incident radiation and temperature per orbit two fixed orbits were considered, with Beta angle of 0° and 75° . Table 2 presents the orbital characteristics of each orbit. For results of variation of Beta angle in time, the orbit presented in Table 2 was initiated for an inclination of 51.3° and Ω de 0° with an initial date of 01/01/2023 at 00:00:00 and propagated through one year.

Table 2. Orbital parameters of the analyzed orbit for beta angle of 0° and 72° .

Date	a	e	Ω	ω	i	β
01/01/2023 00:00:00	500 [km]	0.0	92.3545°	0.0°	51.36°	0.0°
06/14/2023 00:00:00	500 [km]	0.0	160.6734°	0.0°	51.63°	72.0°

3. RESULTS

3.1. Annual variation of beta angle and Radiation

The beta angle variation through 12 months of a 1U CubeSat in LEO orbit can be seen in Figure 3. For 12 months, the beta angle goes from an initial angle of approximately 30° to approximately 0° but it passes by -72° to 72° . Based on Figure 4, several moments of the year where the Beta angle will be 0° can be located. Beta angles of -72° and $+72^\circ$ have analogous incident radiation behavior. beta angles of 0° and 72° were chosen to be analyzed as cases herein to be compared with the work of Morsch Filho et al., (2021).

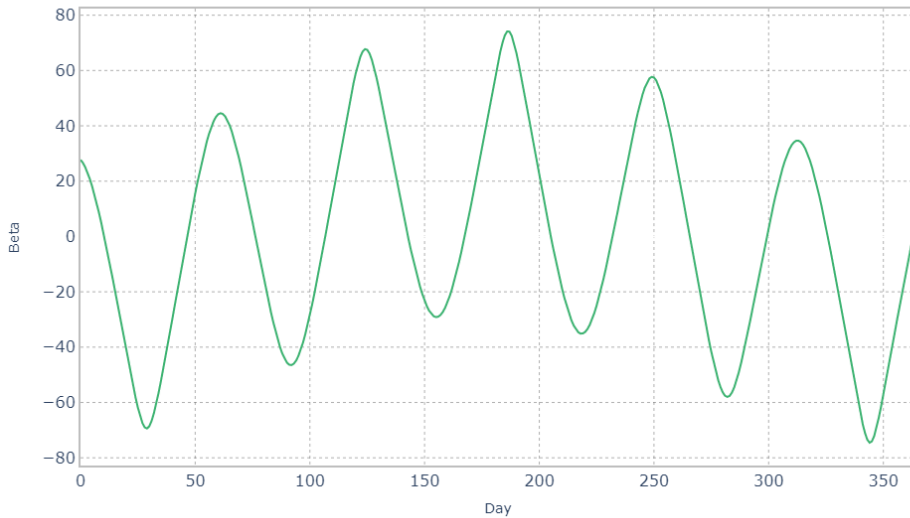


Figure 3: Beta angle variation for the year 2023 for a 1U CubeSat in LEO (inclination of 51.3° with initial date of 01/01/2023 at 00:00:00).

The beta angle variation from 0.0° to 72.0° will impact the amount of total radiation incident on the satellite. Figure 4 shows the amount of maximum, minimum, and average radiation as a function of the beta angle for the satellite with the orbit in Figure 3.

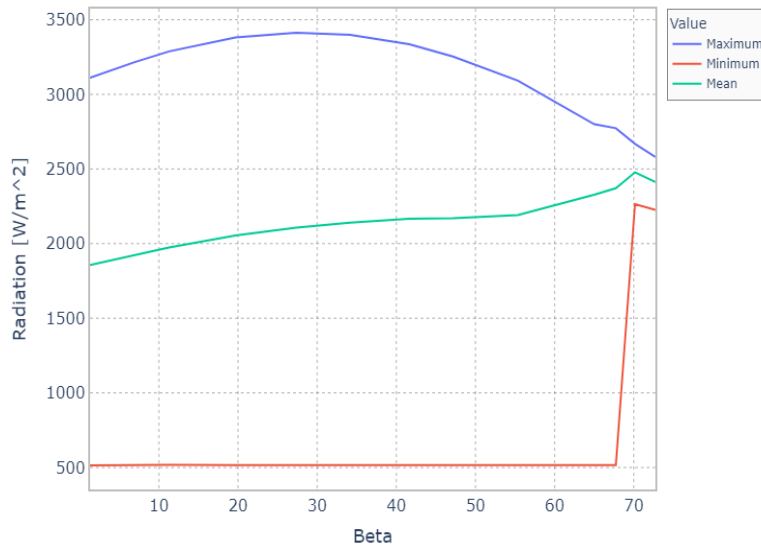


Figure 4: Maximum, minimum, and mean radiation for the beta angle from 0.0° to 72.0°

Figure 4 shows the amounts of maximum, minimum and average total radiation incident on the Cubesat as a function of the beta angle. It is interesting to note that after passing through the 63° beta angle this difference reduces, as the orbit becomes sun-synchronous. With smaller variations in total incident radiation, temperatures will tend to fluctuate less.

3.2. Total incident radiation

The total incident radiation on the satellite for beta angle 0° is indicated for one orbit (approximately 90 min) in Figure 5 (a). The total incident radiation is calculated as the sum of all incident radiation (solar, albedo, and infrared) on all faces of the satellite for each timestep. The Nadir attitude behavior is considered herein (the same face always facing the Earth). For beta 0° an eclipse occurs, where the radiation level is the lowest for this angle reaching a value of 500 W/m². This value represents only the infrared radiation from the Earth. When the satellite exits the shadow of the Earth, the value of incident radiation increases due to direct solar radiation. The oscillation in the total radiation reaching the satellite happens due to the movement of the satellite since the incident radiation then oscillates in each face.

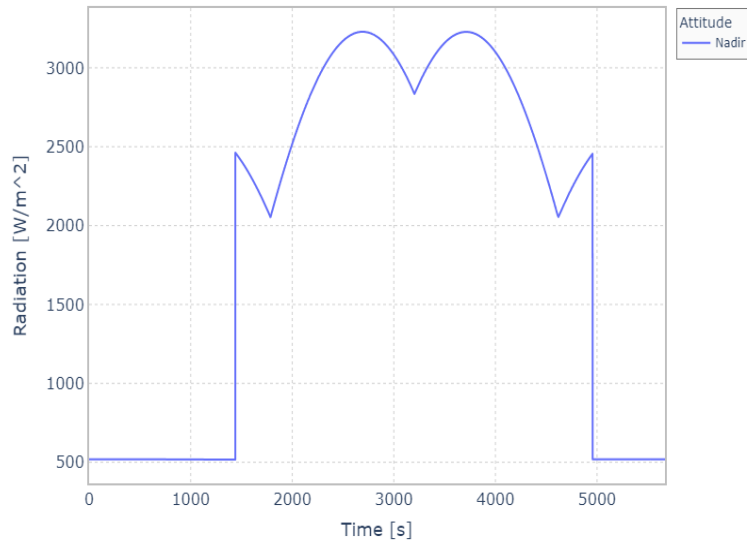


Figure 5. Total incident radiation in the satellite for beta 0.0°.

The same result of total incident radiation is present in Figure 6 for beta 72.0°. For this configuration, the total radiation incident on the satellite varies from 2200 to 2600 W/m² and no eclipse region can be seen. For beta angles bigger than approximately 63°, there is no eclipse region for satellites in LEO. Due to these characteristics, orbits with this beta angle are called sun-synchronous. The variation for beta 72.0° occurs for the regions where there is the incidence of albedo and infrared radiation from the Earth summing to the direct solar radiation. These total radiation results for beta 0° and beta 72° were also observed by the work of Morsch Filho et al. (2021).

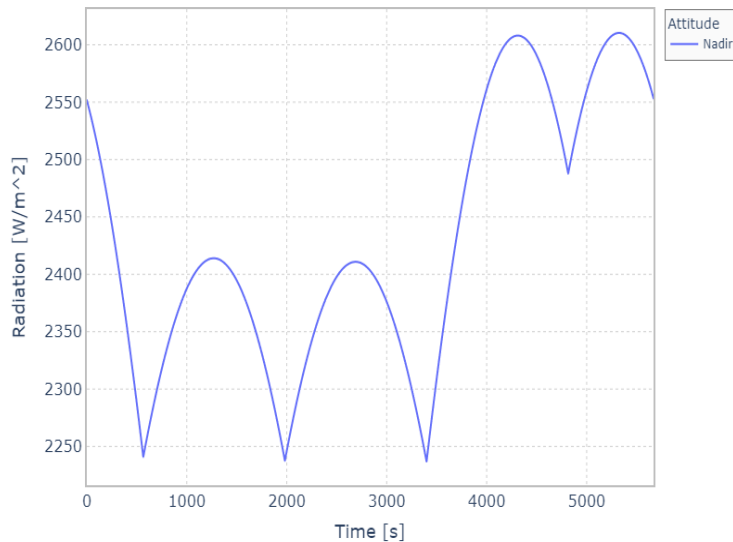


Figure 6. Total incident radiation in the satellite for beta 72.0°.

3.3. Total incident radiation on each face

The total radiation incident on each face for beta 0.0° is presented in Figure 7. The line colors are equivalent to the face color presented in the schematic of the position of the satellite in orbit for each case. Here again, the eclipse region is visible on the value of the incident radiation on each face. Similar results were presented by Morsch Filho et al. (2021). For this Nadir attitude behavior, face 3 (Total 3) is the face always facing the Earth. As expected, faces 1, 2, and 4 (Total 1, Total 2, and Total 4) receive more radiation due to the direct solar radiation incident on these faces. The beta angle variation from 0.0° to 72.0° will impact the amount of total radiation incident on the satellite.

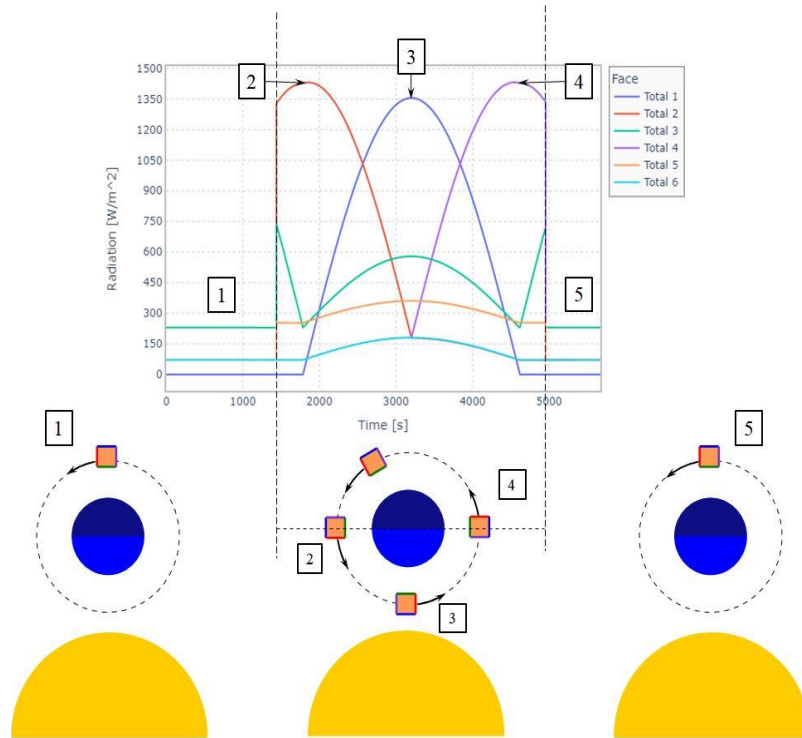


Figure 7: Total incident radiation on each face of the satellite for $\beta 0^\circ$

For $\beta 72^\circ$ (Figure 8) the incident radiation on each face varies significantly from the $\beta 0^\circ$ case. Since this is a sun-synchronous orbit, there is no eclipse region as mentioned before, and all faces, except face 6, have lower incident radiation variation when compared to the $\beta 0^\circ$ case. However, Face 6 has a greater incidence of radiation due to always facing the sun, which could cause elevated temperatures in this face.

In Figure 8, the values marked 1 and 2 represent the satellite behind Earth, and in front of it. As there is no eclipse, the amount of radiation on the upper face is constant, increasing slightly when it passes by 1, as solar radiation adds to the albedo.

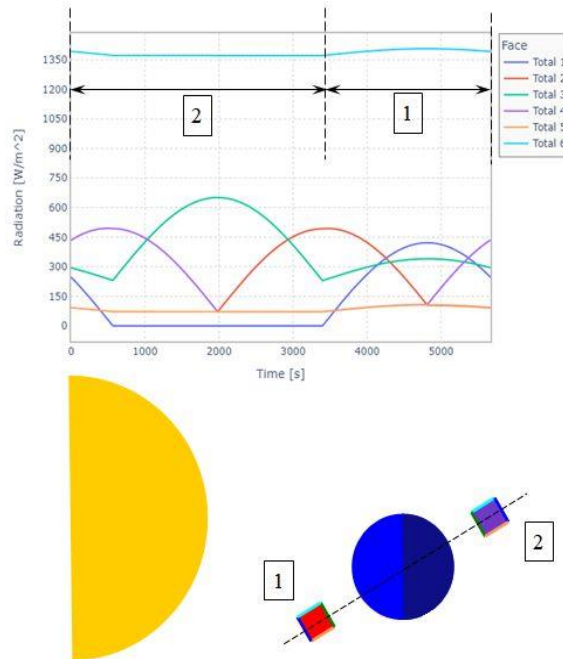


Figure 8: Total incident radiation on each face of the satellite for $\beta 72.0^\circ$

3.4. Temperature Distribution

Applying finite element theory to solve the global resistance model, using data from radiation found after propagating the two orbits of choice, one can find the distribution of temperatures in each component of the 1U Cubesat.

3.4.1. Temperature Distribution for beta 0.0°

The first model presented will be the beta equal to 0.0°. For this angle, the satellite will pass through the planet's shadow, causing the amount of radiation to oscillate as shown in Figure 2. Applying the solution model for finite elements, the following temperature ranges were found for the inner and outer parts of the satellite.

It can be noted that in Figure 9 the temperature distribution follows the same behavior as the radiation shown previously. It is also possible to note that for faces 1, 2, and 4 the maximum temperature increases between the peaks of each face, reaching a maximum of 313 K on face 4. This occurs because the satellite as a whole receives radiation from the 3 main sources, causing the temperature of all components to increase. For faces 3, 5, and 6 the temperatures are lower, as the radiation flux in them is considerably lower (up to 1000 W/m² lower).

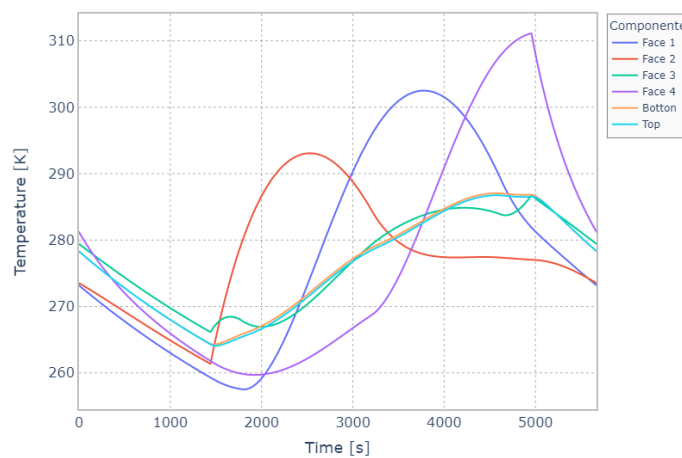


Figure 9. Temperatures for a beta angle of 0.0°

Figure 10 shows the behavior of the satellite PCBs temperatures. It can be noticed that the temperatures of PCBs 1 and 4 fluctuate more than 2 and 3. This is because PCBs 1 and 4 are in contact with the upper part, called the Top, and the lower part, called the Bottom, exchanging heat for each other. radiation and conduction. As the incident radiation on these two faces, Bottom and Top, are close in magnitude, the temperature behaves similarly, even so it is possible to notice a difference, resulting from the heat exchange by conduction of the other components of the satellite. For PCBs 2 and 3, the temperature variation is mainly due to the emission of radiation from the inside of the solar panels, and from the PCBs themselves, as well as the conduction of heat between the screws that hold the structure, making the temperature fluctuate less. It can also be seen that the internal temperatures follow the external temperatures, which in turn are following the incident radiation previously shown.

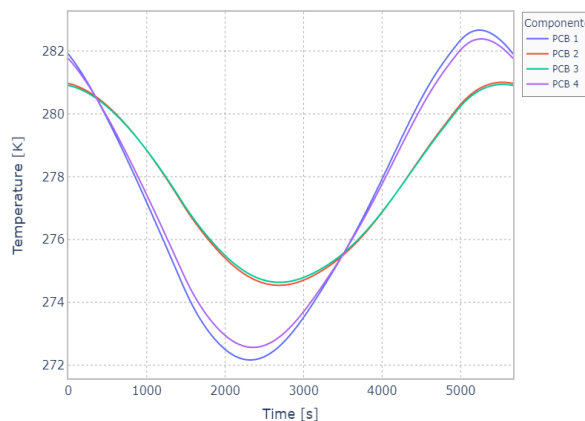


Figure 10. PCBs Temperatures for beta 0.0°

3.4.2. Temperature Distribution for beta 72.0°

Considering the radiation distribution found for the orbit with a beta angle of 72.0°, the following distribution of temperatures was obtained, shown in Figure 11 and Figure 12. Figure 11 shows the temperature variation for the internal and external faces of the CubeSat, while Figure 12 are the temperatures of the PCBs.

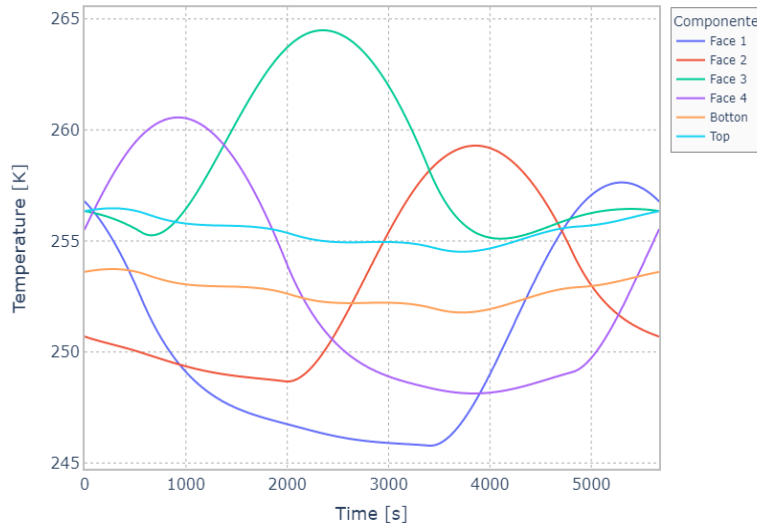


Figure 11. Temperatures for a beta angle of 72°

The temperature behavior for a beta angle of 72° is notably different from that presented for a beta angle of 0.0°. The main difference is that there is not a large temperature oscillation, reaching a maximum of 12°C on face 2. It is also noted that the temperatures in the upper and lower parts almost do not oscillate, and have a similar behavior, however, the temperature at the top is larger than at the bottom. This occurs because, in the incident radiation model, the upper part is in direct contact with solar radiation, while the lower part receives only a small portion of albedo and infrared radiation. Although the amount of radiation is so different between both faces, the emissivity and absorptivity considered in the model are small (ϵ of 0.3 and α of 0.13), making the temperature not so high at the top and not so low at the bottom.

The distribution of temperatures varies according to the incident radiation at the top and bottom, mainly. Note that the temperature range is greater in PCB 1 and reduces to PCB 4, as the radiation incident on the upper part is greater, and the heat is conducted by the screws and emitted between the PCBs. The inner part of the panels also emits radiation, causing the temperature to fluctuate.

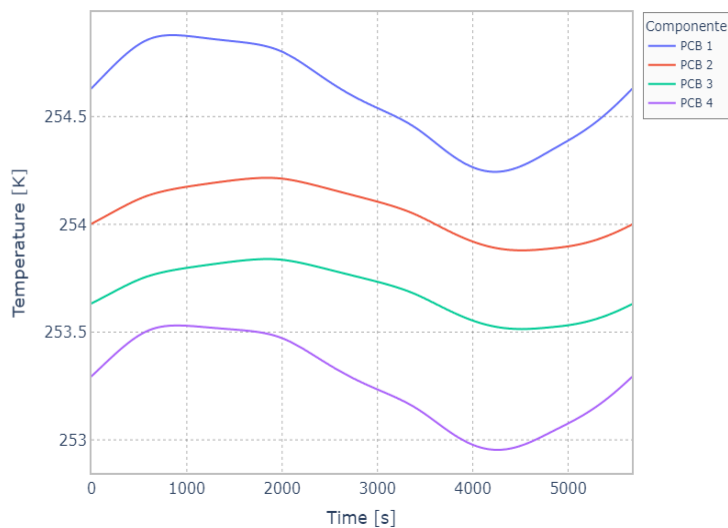


Figure 12. PCBs Temperatures for beta 72.0°

4. Conclusion

The correct determination of the temperature variation in orbital platforms is essential for the lifetime of the satellite in orbit to be completed. The operating conditions must be correctly determined, as unexpected temperature variations can cause a complete failure of the systems. The thermal design is essential, but the use of robust programs turns out to be unfeasible for low-cost projects, such as CubeSats projects, for that, simplified models are used to determine the temperature of the internal and external components of the satellites.

From the development of an orbital and thermal model, it is possible to determine whether the satellite components will survive the temperature variations caused by the radiation variations that occur naturally due to orbital perturbations. For this, the two cases with a maximum and minimum beta angle were chosen to demonstrate such variation.

The findings reveal that eclipses exert a profound influence on temperature distribution, amplifying the contrast between maximum and minimum temperatures on the lateral faces by as much as 50°C. Conversely, in a sun-synchronous orbit, this disparity narrows significantly, reducing it to a mere 12°C. Internal temperatures similarly underwent substantial alterations: whereas at a beta angle of 0.0°, temperatures exhibited substantial fluctuations, at a beta angle of 72°, the behavior remained consistent across the PCBs, with variations limited to the temperature range.

5. ACKNOWLEDGMENTS

We would like to express our gratitude to the Brazilian Space Agency for their support of the project and guidance for this work and to the Santa Catarina Parliamentary Bench for the financial support for the development of the Catarina Constellation.

6. REFERENCES

- Ali, A., Ullah, K., Rehman, H.U., Bari, I. and Reyneri, L.M., 2017. "Thermal characterization analysis and modeling techniques for CubeSat-sized spacecraft". *The Aeronautical Journal*, Vol. 121, No. 1246, p. 1858–1878. doi: 10.1017/aer.2017.108.
- Bonnici, M., Mollicone, P., Fenech, M. and Azzopardi, M.A., 2019. "Analytical and numerical models for thermal related design of a new pico-satellite". *Applied Thermal Engineering*, Vol. 159, p. 113908.
- Bousedra, K., 2023. "Downstream space activities in the new space era: Paradigm shift and evaluation challenges". *Space Policy*, Vol. 64, p. 101553.
- Capderou, M., 2014. *Handbook of Satellites Orbits*. Springer, Paris, first edition.
- Curtis, H.D., 2014. *Orbital Mechanics for Engineering Students*. Butterworth-Heinemann, Boston, third edition.
- Garzón, A., Tami, J.A., Campos-Julca, C.D. and Acero-Niño, I.F., 2022. "Effect of beta angle and contact conductances on the temperature distribution of a 3u CubeSat". *Thermal Science and Engineering Progress*, Vol. 29, p. 101183.
- Gilmore, D.G., 2002. "Spacecraft thermal control handbook, volume i: Fundamental technologies".
- Morsch Filho, E., Seman, L.O. and de Paulo Nicolau, V., 2021. "Simulation of a CubeSat with internal heat transfer using finite volume method". *Applied Thermal Engineering*, Vol. 193, p. 117039.
- Nogueira, P., 2017. *Micro-Satellite Electrical Power Subsystem Design and Test for LEO Mission*. Electrical Engineering master's degree, International School, Pequim.
- Olatunji, J., Acheson, C., Szmigiel, M., Wimbush, S. and Long, N., 2022. "Orbital and thermal modeling of a 3u CubeSat equipped with a high-temperature superconducting coil". *Acta Astronautica*, Vol. 190, pp. 413–429.
- Paravano, A., Locatelli, G. and Trucco, P., 2023. "What is value in the new space economy? the end-users perspective on satellite data and solutions". *Acta Astronautica*, Vol. 210, p. 554–563.
- Picone, J., Hedin, A., Drob, D. and Aikin, A., 2002. "Nrlmsise-00 empirical model of the atmosphere: Statistical comparison and scientific issues". *Journal of Geophysical Research*, Vol. 107, p. 16.
- Tucker, B.P. and Alewine, H.C., 2023. "Everybody's business to know about space: Cross-disciplinarity and the challenges of the new space age". *Space Policy*.
- Villela, T., Costa, C.A., Brandão, A.M., Bueno, F.T. and Leonardi, R., 2019. "Towards the thousandth CubeSat: A statistical overview". *International Journal of Aerospace Engineering*, Vol. 2019, p. 5063145.

4. RESPONSIBILITY NOTICE

The authors are the only ones responsible for the printed material included in this paper.